Int. J. Advanced Design and Manufacturing Technology, 2023, Vol. 16, No. 3, pp. 1-8

DOI: 10.30486/admt.2023.1968678.1385 ISSN: 2252-0406 https://admt.isfahan.iau.ir

Investigating Effects of Vertical Baffles on Damping of Shallow Water Sloshing using a 3D Model

Rahim Shamsoddini[1]
Department of Mechanical Engineering,
Sirjan University of Technology, Sirjan, Iran
E-mail: shamsoddini@sirjantech.ac.ir

Bahador Abolpour[2, *]
Department of Chemical Engineering,
Sirjan University of Technology, Sirjan, Iran
E-mail: bahadorabolpor1364@yahoo.com
*Corresponding author

Received:2 September 2022, Revised: 31 January 2023, Accepted:21 February 2023

Abstract: Liquid sloshing is a common phenomenon in the transporting of liquid tanks. A safe liquid transporting needs to control the entered fluctuating forces to the tank walls, before leading these forces to large forces and momentums. Using predesigned baffles is a simple method for solving this problem. Smoothed Particle Hydrodynamics is a Lagrangian method that has been widely used to model such phenomena. In the present study, a three-dimensional incompressible SPH model has been developed for simulating the liquid sloshing phenomenon. This model has been improved using the kernel gradient correction tensors, particle shifting algorithms, turbulence model, and free surface particle detectors. The results of the three-dimensional numerical model are compared with an experimental model, showing the very good accuracy of the three-dimensional numerical method used. This study aims to investigate vertical baffle effects on the control and damping of liquid sloshing. The results of the present investigation show that in this particular case, by using baffles, it is possible to reduce more than 50% of the maximum value of pressure fluctuations in the slashing phenomenon.

Keywords: Free Surface, Shallow Water Sloshing, SPH, Vertical Baffle

Biographical notes: Rahim Shamsoddini received his PhD in Mechanical Engineering from University of Yazd in 2014. He is currently Associate Professor at the Department of Mechanical Engineering, Sirjan University of Technology, Sirjan, Iran. His current research interest includes CFD, SPH in Newtonian and non-Newtonian fluid flows. **Bahador Abolpur** is Associate Professor of Chemical engineering at the Sirjan University of Technology, Sirjan, Iran. He received his PhD in Chemical engineering from Shahid Bahonar University of Kerman in 2013.

Research paper

1 INTRODUCTION

The motion of liquids in vessels and containers, called sloshing, widely occurred in various industrial systems. In the sloshing, the motion of the structure is transmitted to the liquid. An important problem in the free surface flows is the liquid sloshing in the tanks. It is a well-known phenomenon in liquid tanks. The sloshing phenomenon may create great forces and momentums, so in this sense, safe transporting of the tank and its carrier may be difficult. Hence, predicting and controlling their behaviors are essential requirements in the liquid transport industries.

In the past, the Eulerian methods were used to model two-phase flows. These methods are usually grid-based, therefore the motion of a solid body should be defined and imposed at any iteration. Modeling of the free surface is another challenge of the grid-based models. Recently, the Lagrangian and mesh-free methods, such as Smoothed Particle Hydrodynamics (SPH), have been also used for modeling the sloshing phenomenon. SPH was introduced by Lucy [1], Gingold, and Monaghan [2] in 1977. In 1982, Gingold and Monaghan [3] used this method in the simulation of a compressible and inviscid flow. In 1997, Morris et al. [4] used SPH for modeling an incompressible flow. Modeling of Newtonian [5-6], and non-Newtonian flows [7-8], free-surface flow [9], two-phase flow [9-10], mixing flow [11-14], and Fluid-Structure Interaction (FSI) problems [7], [15], are examples of SPH applications. Weakly Compressible Smoothed Particle Hydrodynamics (WCSPH) and Incompressible SPH (ISPH) are two well-known SPH methods. The WCSPH method uses an Equation of state for estimating the pressure, while the ISPH method solves the Poisson Equation to determine this quantity. In this study, an ISPH algorithm has been used for modeling a one-way coupled FSI problem with free-surface flow. The SPH encounters special problems: particle clustering, defects, and tensile instability; to cover these problems, the advanced discretization style and shifting algorithms are used. In addition, turbulence modeling, and free surface particle detecting are the other two major parts of the present model. This method was also assessed with the experimental results. Because of the Lagrangian and meshless nature, the SPH can model free surface flows, easily. Rostami Varnousfaaderani and Ketabdari [16] modified the WCSPH method for simulating a two-dimensional plunging solitary wave breaking process. Violeau and Issa [17] examined different turbulence models for the SPH simulations. Omidvar and Nikeghbali [18] used the SPH method for simulating the dam-break propagation over an erodible bed and sediment distribution beneath. These researchers [16-18] used the WCSPH method. However, this method is undermined by non-physical fluctuations in the density field. The ISPH treats the WCSPH method [19], but recent efforts reduced the non-physical fluctuations [5], [7]. There is extensive research in this field. Kim et al. [20] had a comparative study on model-scale sloshing. Zou et al. [21] studied the effect of liquid viscosity on sloshing using a set of experiments. Hou et al. [22] simulated liquid sloshing behavior in a two-dimensional rectangular tank using the ANSYS-FLUENT software. Godderidge et al. [23] modeled sloshing flow in a rectangular tank using a commercial Computational Fluid Dynamic (CFD) code. SPH is also a convenient method in the simulation of liquid sloshing. There are also some researches in this field, which used the SPH method [24-28].

As evident in the review of past studies, it is rare to find numerical work in this field that considers three-dimensional effects in the simulation of shallow water sloshing. One of the other strengths of the present work is the simultaneous comparison of experimental and numerical results during the research, which in addition to measuring the accuracy, the capabilities of each method can be used. One strategy to reduce sloshing fluctuation is the use of a baffle mechanism. Therefore, in this study, a robust modified explicit ISPH method has been developed and applied for simulating the shallow water sloshing phenomenon in a rectangular box. The method has been improved using the kernel gradient correction, free surface particle detector, turbulent model, and particle shifting algorithm. Simultaneously, an experimental mechanism has been designed and constructed to record the shallow water sloshing details. The comparison between the numerical and experimental results approves the ability of this model to predict the behaviors of the sloshing phenomenon. This study aims to investigate the effects of vertical baffles on the controlling of the shallow water sloshing phenomenon. Therefore, in the following, first, the numerical method and algorithm are introduced, next, the experimental setup is explained, and then the results are discussed.

2 NUMERICAL PROCEDURES

SPH has been based on an integral approximation. This integral form and its summation approximation on the discrete points have been presented below:

$$f(r) = \int_{\Omega} f(r')W(r-r',h)dr' = \sum_{j} \forall_j f_j W(r-r_j,h) \quad (1)$$

After examination of different kernel functions, it has resulted that [29], the fifth-order Wendland kernel function, with the following relation, is accurate for modeling fluid flow:

$$W(r,h)=W_0\times\begin{cases}\left(1-\dfrac{|r|}{h}\right)^4\left(4\dfrac{|r|}{h}+1\right) & 0\le\dfrac{|r|}{h}<1\\ 0 & \dfrac{|r|}{h}\ge 1\end{cases} \quad (2)$$

The governing Equations are momentum and pressure Poisson Equations, as follows:

$$\frac{d\boldsymbol{V}}{dt}=\nu\nabla^2\boldsymbol{V}+\boldsymbol{g}-\frac{\nabla p}{\rho}+\frac{\nabla.\tau_t}{\rho} \quad (3)$$

$$\nabla.\left(\frac{1}{\rho}\nabla p^{n+1}\right)_i=\frac{\nabla.\boldsymbol{V}_i^{*,n+1}}{\Delta t} \quad (4)$$

This algorithm was developed to model special problems with the effects of free surface and forced motion of solid boundaries. In order to overcome the SPH defects, some modifications have been considered. The present three-dimensional modeling contains the above main body and the following sub-algorithms:

- The forced motion of structures
- Free surface detectors
- Turbulence viscosity calculators
- Shifting algorithms

In this algorithm, a predictor-corrector scheme has been implemented. In the first step, according to the gravitational, viscous, and turbulence terms of the momentum Equation, the velocity is predicted as below [4]:

$$\boldsymbol{V}_i^{*,n+1}=\boldsymbol{V}_i^n+\left(\boldsymbol{g}+\sum_j 2\nu\forall_j\frac{\boldsymbol{V}_i-\boldsymbol{V}_j}{r_{ij}}\boldsymbol{e}_{ij}.\left(\boldsymbol{B}_i.\nabla W_{ij}\right)+\sum_j m_j\left(\frac{\tau_{t_i}}{\rho_i^2}+\frac{\tau_{t_j}}{\rho_j^2}\right).\nabla W_{ij}\right)\Delta t \quad (5)$$

Where, $\tau_t=2\mu_t S_{ij}$, in which $\mu_t=\rho(C_s\delta)|\bar{S}|$ [31-32], and S is the strain rate. After calculation of the intermediate velocity, the pressure is calculated using "Eq. (4)", as below:

$$\sum_j 2\frac{\forall_j}{\rho_{ij}}\frac{p_i^{n+1}-p_j^{n+1}}{r_{ij}}\boldsymbol{e}_{ij}.\left(\boldsymbol{B}_i.\nabla W_{ij}\right)=\frac{\left\langle\nabla.\boldsymbol{V}_i^{*,n+1}\right\rangle}{\Delta t} \quad (6)$$

In this study, the above Equation has been explicitly solved as below:

$$\left(P_i^{n+1}\right)^{k+1}=\left(\frac{\left(\sum_j 2\frac{\forall_j}{\rho}\frac{p_j^{n+1}}{r_{ij}}\boldsymbol{e}_{ij}.\left(\boldsymbol{B}_i.\nabla W_{ij}\right)+\frac{1}{\Delta t}\sum_j\forall_j\left(\boldsymbol{V}_j^{*,n+1}-\boldsymbol{V}_i^{*,n+1}\right).\left(\boldsymbol{B}_i.\nabla W_{ij}\right)\right)}{\sum_j 2\frac{\forall_j}{\rho r_{ij}}\boldsymbol{e}_{ij}.\left(\boldsymbol{B}_i.\nabla W_{ij}\right)}\right)^k \quad (7)$$

If the ith particle is located on the free surface, pi is set to zero. To detect free surface particles, a sub-algorithm has been developed. For each particle, $\nabla.\boldsymbol{r}$ is calculated. For the three-dimensional cases, $\nabla.\boldsymbol{r}=3.0$, the SPH discretization of $\nabla.\boldsymbol{r}$ would be:

$$\left\langle\nabla.\boldsymbol{r}\right\rangle_i=\sum_j\forall_j\left(\boldsymbol{r}_j-\boldsymbol{r}_i\right).\nabla W_{ij} \quad (8)$$

However, $\nabla.\boldsymbol{r}$ would be less than 3 for the free surface particles. In addition, all particles $\nabla.\boldsymbol{r}<2.7$ can be considered free surface particles. After calculating pressure, velocity is corrected as below:

$$\boldsymbol{V}_i^{n+1}=\boldsymbol{V}_i^{*,n+1}-\left\langle\frac{\nabla p}{\rho}\right\rangle_i^{n+1}\Delta t \quad (9)$$

Another utilized sub-algorithm is the definition of force motion of solid bodies. In this section, the formulation of particle motion has been defined. For all particles, the new position is calculated using the following relation:

$$\boldsymbol{r}_i^{n+1}=\boldsymbol{r}_i^n+\boldsymbol{V}_i^{n+1}\Delta t \quad (10)$$

Defects, tensile instability, and clustering distributions are complications of the SPH modeling. To prevent them, a shifting algorithm has been used, similar to the Shamsoddini et al. method [11-13]. First, $\Delta\boldsymbol{r}_i$ is calculated as the shifting particle vector, i.e. $\Delta\boldsymbol{r}_i=\varepsilon\bar{\boldsymbol{r}}_i$, where $\bar{\boldsymbol{r}}_i=\sum_j\forall_j\boldsymbol{r}_{ij}W_{ij}$. Homogeneous distribution of the particles around the particle i leads to $\bar{\boldsymbol{r}}_i=0$. If $\bar{\boldsymbol{r}}_i\neq 0$, then the particle is shifted by $\Delta\boldsymbol{r}_i$. Now, it is necessary to correct the flow field variables in the new position, according to the first-order Taylor series expansion, as follows:

$$\Delta\boldsymbol{V}_i=\Delta\boldsymbol{r}_i.\left\langle\nabla\boldsymbol{V}\right\rangle_i \quad (11)$$

$$\Delta p_i=\rho_i\Delta\boldsymbol{r}_i.\left\langle\frac{\nabla p}{\rho}\right\rangle_i \quad (12)$$

Near each wall boundary, two rows of dummy particles are arranged. The velocity of each dummy particle is calculated attending to its corresponding particle. If the wall has no/or linear motion, the velocity of the dummy particle is the same as its corresponding wall particle. For rotational cases, the angular velocity of the dummy particles and wall particles are the same. The pressure Equation for dummy particle is obtained using dot multiplying the normal vector of the surface to the momentum Equation, as below:

$$\left(\frac{\nabla p}{\rho}\right).\boldsymbol{n}_w = \frac{1}{\rho}\frac{\partial p}{\partial n_w} = -\frac{d\boldsymbol{V}_{b_i}}{dt}.\boldsymbol{n}_w + \nabla.\left(\nu_e \nabla \boldsymbol{V}\right).\boldsymbol{n}_w + \boldsymbol{g}.\boldsymbol{n}_w \qquad (13)$$

Because of the no-slip condition of the dummy particles, this Equation can be discretized according to the finite difference method, as below:

$$p_i^{n+1} = p_i^n + \rho\delta_n\left(-\frac{d\boldsymbol{V}_{b_i}}{dt}.\boldsymbol{n}_w + \nabla.\left(\nu_e \nabla \boldsymbol{V}\right).\boldsymbol{n}_w + \boldsymbol{g}.\boldsymbol{n}_w\right)_i^n \qquad (14)$$

In many cases, the second term of the right side of this Equation is small enough for neglect. If the wall velocity is constant, the Equation is converted to the Neumann condition for pressure.

The presented algorithm has been used for modeling a fluid flow with the free surface engaged in moving rigid bodies. In the following, the accuracy of the present algorithm is evaluated using the experimental data. In the next section, the experimental setup is explained and then the numerical and experimental results are compared.

3 EXPERIMENTS

The experimental setup consisted of an electrical motor, a crank mechanism, a glass box (14×41×20 cm3) mounted on four wheels, which has been shown in "Fig.1".

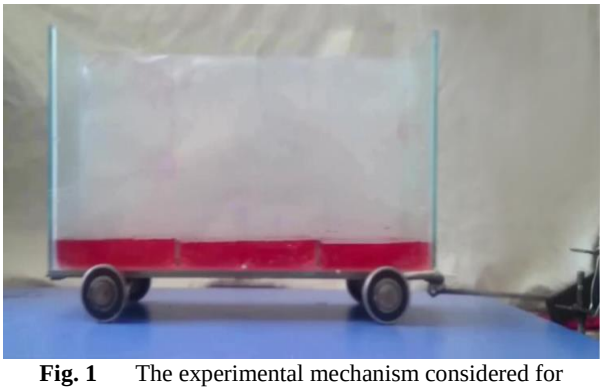

Fig. 1 The experimental mechanism considered for investigating the effect of baffles on the shallow water sloshing phenomenon.

First, the crank and the slider were connected to the engine, then, the glass box was set on a cart (with four wheels), finally, the cart was attached to the crank. The engine was set to a certain rpm. The glass box was filled with water to the height of 2.5 cm. A charge-coupled device (CCD) camera with 21MPixel was used to take the experimental pictures. Three cases were adjusted:

- a baffle-less box
- a box with one vertical baffle
- a box with two vertical baffles

Figure 1 shows the box with two 2.2 cm height baffles. The distance between each baffle and the nearest wall is equal to one-third of the length of the tank. The aperiodic motion was considered for the tank, in the experiments. Therefore, this tank had a horizontal oscillation with a certain frequency and domain. This motion was transmitted to the water, which made the liquid flow toward the right and left sides.

4 RESULTS AND DISCUSSION

Liquid motion in the tanks under vibration conditions is an interesting problem. Modelling this problem has useful results for predicting the sloshing phenomenon in the containers. After an investigation on the particle size, it has been estimated that the particle size with $\delta/L=0.0085$ is proper for numerical modelling. In the present study, vertical baffles were tested to control the violence of water flow, numerically and experimentally. In all studied cases, the results of the numerical simulation are compared with the experimental results. It is observed that there is a proper agreement between the numerical and experimental results. Figure 2 shows both the numerical and experimental results.

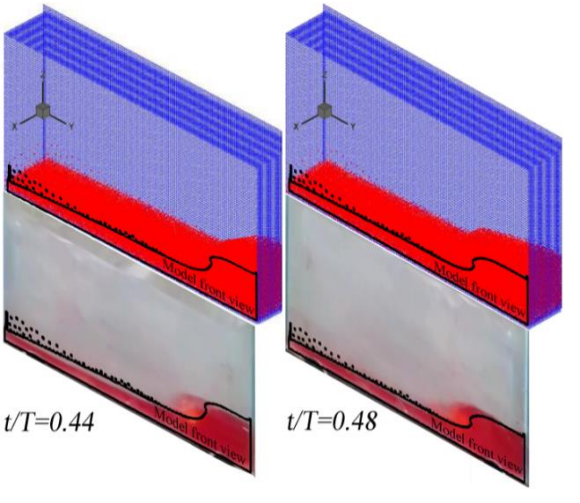

A continuous fluid flow is observed along the horizontal surface of the box until the liquid reaches a vertical wall. Then, the liquid goes up along this wall. After that, the liquid returns and is accumulated. This violent flow is observed in the numerical run and experimental test, similarly, as shown in "Fig. 2". This flow creates collapses of water on the vertical walls, frequently, and high amplitude forces with high wave height, subsequently. If the wave height is controlled, the force domain is also controlled. For this purpose, a vertical baffle (with 2.2 cm height), which was set in the middle of the horizontal bottom surface of the box, was tested.

The numerical and experimental results of this case have been shown in “Fig. 3”. Comparing the presented results in “Figs. 2 and 3” demonstrates that, the presence of this baffle reduces the height of the generated wave and also the collapse of water on the vertical walls, significantly.

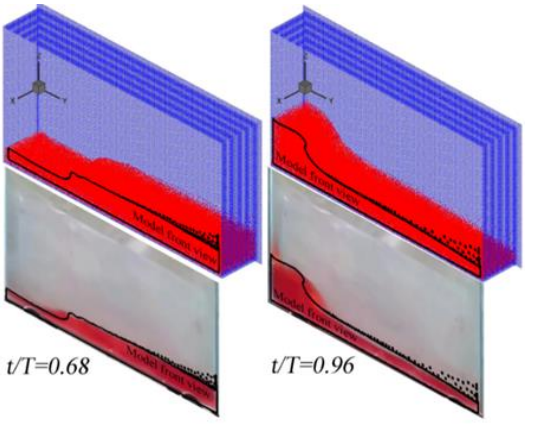

Fig. 2 Shallow-water sloshing in the rectangular for different times of the motion, a comparison between the presented SPH simulation and experimental results.

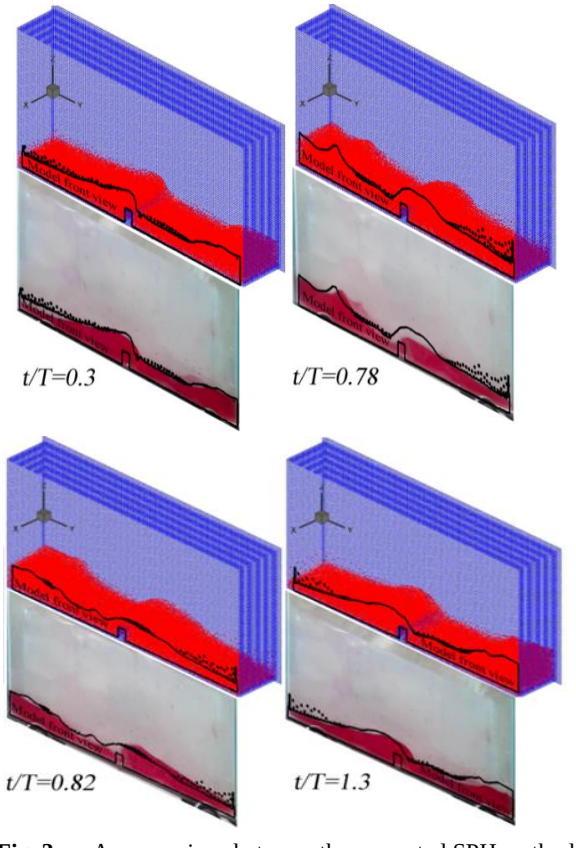

Fig. 3 A comparison between the presented SPH method (left) and experimental results (right) for variation of the free surface of shallow water sloshing phenomena at different times of the periodic motion, in the presence of a vertical baffle.

Now, it is expected that the maximum wave height has a more reduction with increasing the number of baffles. Therefore, two vertical baffles, which were set in each one-third of the bottom surface length, were tested. The results of the water sloshing in the presence of these baffles have been shown in “Fig. 4”. The maximum height of the waves is reduced in comparison with the zero and one baffle tanks, considerably.

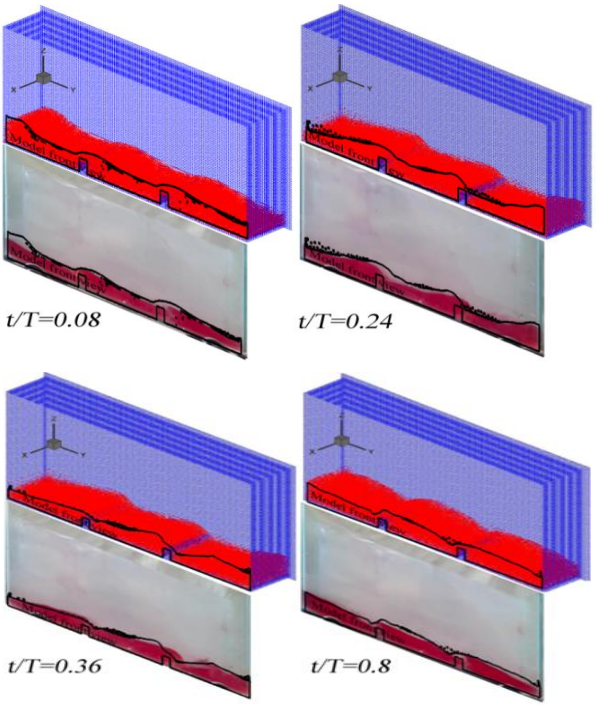

Fig. 4 A comparison between the presented SPH method (left) and experimental results (right) for variation of the free surface of shallow water sloshing phenomena at different times of the periodic motion, in the presence of two vertical baffles.

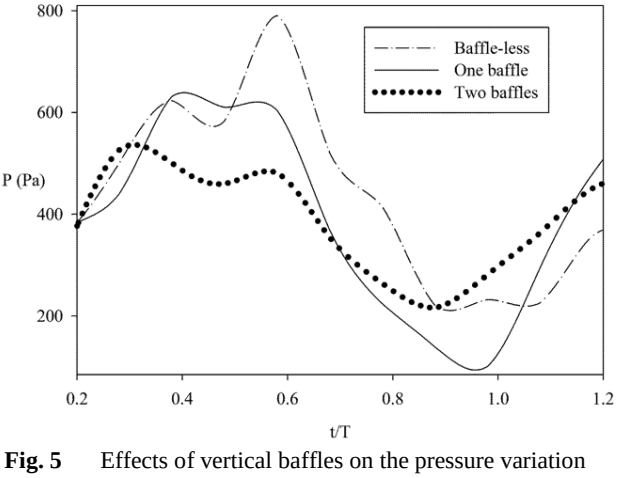

Fig. 5 Effects of vertical baffles on the pressure variation at the right-bottom corner of the box.

Figure 5 presents a quantitative comparison among these three cases. This Figure shows the calculated time variation of the pressure at the right-bottom center of the box. It has resulted that, the pressure variation of this point is a periodic function of time. The force sinusoidal motion of the tank is transmitted to the fluid, gradually. Therefore, a periodic flow is provided in the tank. As depicted, increasing the baffles number decreases the pressure variations, considerably. At this point, the pressure variations domain has been reduced by about 53% for the tanks with two baffles in comparison with the baffle-less tank.

5 CONCLUSIONS

In the presented study, a robust modified explicit 3D ISPH method was developed for simulating the shallow water sloshing phenomena in a rectangular box. This method was improved using the kernel gradient correction, free surface particle detector, turbulent model, and particle shifting algorithm. Simultaneously, a mechanism was designed and constructed to record the shallow water sloshing details, experimentally. The comparison between the numerical and experimental results approved the accuracy of the presented algorithm for modeling this phenomenon. The effects of the vertical baffle on controlling the shallow water sloshing phenomenon were investigated in this study. For this purpose, two tanks, with one and two vertical baffles, were compared with a baffle-less tank, numerically and experimentally. The results have shown that the presence of the vertical baffles has an essential role in the reduction of the sloshing fluctuations.

6 NOMENCLATURES

A	The domain of the periodic motion of the experiment tank (*0.045 m*)
$\boldsymbol{B_i}$	The kernel gradient corrective tensor [30]: $\boldsymbol{B}_i = -\left[\sum_j \forall_j \boldsymbol{r}_{ij} \nabla W_{ij}\right]^{-1}$.
c_s	Constant (equal to 0.2) [31, 32]
$\boldsymbol{e}_{ij}$	The unit vector (from j^{th} particle to i^{th} particle)
g	The gravitational acceleration
h	Smoothing length
n_w	The normal vector of the surface
p	Pressure
r	Position vector
r'	Sub-integral variable
S_{ij}	The strain rate of the mean flow: $S_{ij} = \frac{1}{2}\left(\frac{\partial u_i}{\partial x_j} + \frac{\partial u_j}{\partial x_i}\right)$
t	Time
T	Period of the motion of the experiment tank (*1 Sec*)
V	Fluid velocity
$\boldsymbol{V}_i^{*,n+1}$	Intermediate velocity
W	The Kernel function
W_0	A function of smoothing length as $\frac{21}{2\pi h^3}$ for three-dimensional problems
x	The horizontal position of the tank
δ	Particle spacing
δ_n	The distance between the dummy particles and corresponding wall particles
ε	A constant varying between 0 and 0.1
μ_t	Turbulent dynamic viscosity of the fluid
ρ	The density of the fluid
τ_t	Turbulent stress tensor: $\tau_t = 2\mu_t S_{ij}$
υ	Kinematicviscosity of the fluid
ν_t	Turbulent viscosity [31-32]: $\nu_t = (c_s\delta)^2\left\|\bar{S}\right\|$,
$\forall_j$	The volume of j^{th} particle

REFERENCES

[1] Lucy, L. B., A Numerical Approach to The Testing of The Fission Hypothesis, Astronomical Journal, Vol. 82, 1977, pp. 1013-1024.

[2] Gingold, R. A., Monaghan, J. J., Smoothed Particle Hydrodynamics: Theory and Application to Non-Spherical Stars, Monthly Notices of the Royal Astronomical Society, Vol. 181, No. 3, 1977, pp. 375–389.

[3] Gingold, R. A., Monaghan, J. J., Kernel Estimates as A Basis for General Particle Methods in Hydrodynamics, Journal of Computational Physics, Vol. 46, No. 3, 1982, pp. 429-453.

[4] Morris, J. P., Fox, P. J., and Zhu, Y., Modeling Low Reynolds Number Incompressible Flows Using SPH, Journal of Computational Physics, Vol. 136, No. 1, 1997, pp. 214-226.

[5] Sefid, M., Fatehi, R., and Shamsoddini, R., A Modified Smoothed Particle Hydrodynamics Scheme to Model the Stationary and Moving Boundary Problems for Newtonian Fluid Flows, ASME Journal of Fluids Engineering, Vol. 137, No. 3, 2015, pp. 031201-9.

[6] Shadloo, M. S., Zainali, A., Sadek, S. H., and Yildiz, M., Improved Incompressible Smoothed Particle

Hydrodynamics Method for Simulating Flow Around Bluff Bodies, Computer Methods in Applied Mechanics and Engineering, Vol. 200, No. 9-12, 2011, pp. 1008-1020.

[7] Hashemi, M. R., Fatehi, R., and Manzari, M. T., SPH Simulation of Interacting Solid Bodies Suspended in A Shear Flow of An Oldroyd-B Fluid, Journal of Non-Newtonian Fluid Mechanics, Vol. 166, No. 21-22, 2011, pp. 239-1252.

[8] Shamsoddini, R., Aminizadeh, and N., Sefid, M., An Improved WCSPH Method To Simulate the Non-Newtonian Power-Law Fluid Flow Induced by Motion of a Square Cylinder, CMES-Computer Modeling in Engineering & Sciences, Vol. 105, No. 3, 2015, pp. 209-230.

[9] Farrokhpanah, A., Samareh, B., Rentschler, and Mostaghimi, J., Applying Contact Angle to A Two-Dimensional Multiphase Smoothed Particle Hydrodynamics Model, ASME Journal of Fluids, Vol. 137, No. 4, 2015, pp. 041303-12.

[10] Shadloo, M. S., Zainali, A., and Yildiz, M., Simulation of Single Mode Rayleigh–Taylor Instability by SPH Method, Computational Mechanics, Vol. 51, No. 5, 2013, pp. 699-715.

[11] Shamsoddini, R., Sefid, M., and Fatehi, R., Lagrangian Simulation and Analysis of The Micromixing Phenomena in A Cylindrical Paddle Mixer Using a Modified Weakly Compressible Smoothed Particle Hydrodynamics Method, Asia-Pacific Journal of Chemical Engineering, Vol. 10, No. 1, 2015, pp. 112-122.

[12] Shamsoddini, R., Sefid, M., and Fatehi, R., ISPH Modelling and Analysis of Fluid Mixing in A Microchannel with An Oscillating or A Rotating Stirrer, Engineering Applications of Computational Fluid Mechanics, Vol. 8, No. 2, 2014, pp. 289-298.

[13] Shamsoddini, R., Sefid, M., Lagrangian Simulation and Analysis of The Power-Law Fluid Mixing in The Two-Blade Circular Mixers Using a Modified WCSPH Method, Polish Journal of Chemical Technology, Vol. 17, No. 2, 2015, pp. 1-10.

[14] Shamsoddini, R., Sefid, M., and Fatehi, R., Incompressible SPH Modeling and Analysis of Non-Newtonian Power-Law Fluids, Mixing in A Microchannel with An Oscillating Stirrer, Journal of Mechanical Science and Technology, Vol. 30, No. 1, 2016, pp. 307-316.

[15] Hashemi, M. R., Fatehi, R., and Manzari, M. T., A Modified SPH Method for Simulating Motion of Rigid Bodies in Newtonian Fluid Flows, International Journal of Non-Linear Mechanics, Vol. 47, No. 6, 2012, pp. 626-638.

[16] Rostami, V. M., Ketabdari, M. J., Numerical Simulation of Solitary Wave Breaking and Impact on Seawall Using a Modified Turbulence Sph Method with Riemann Solvers, Journal of Marine Science and Technology, Vol. 20, No. 2, 2015, pp. 344-356.

[17] Violeau, D., Issa, R., Numerical Modelling of Complex Turbulent Free-Surface Flows with The SPH Method: An Overview, International Journal for Numerical Methods in Fluids, Vol. 53, No. 2, 2007, pp. 277–304.

[18] Omidvar, P., Nikeghbali, P., Simulation of Violent Water Flows Over a Movable Bed Using Smoothed Particle Hydrodynamics, Journal of Marine Science and Technology, Vol. 22, No. 2, 2017, pp. 270-287.

[19] Lee, E. S., Moulinec, C., Xu, R., Violeau, D., Laurence, D., and Stansby, P., Comparisons of Weakly Compressible and Truly Incompressible Algorithms for the SPH Mesh Free Particle Method, Journal of Computational Physics, Vol. 227, No. 18, 2008, pp. 8417–8436.

[20] Kim, S. Y., Kim, K. H., Trudell, R. W., and Kim, Y., Comparative Study on Model-Scale Sloshing Tests, Journal of Marine Science and Technology, Vol. 17, No. 1, 2012, pp. 47-58.

[21] Zou, C. F., Wang, D. Y., Cai, Z. H., and Li, Z., The Effect of Liquid Viscosity on Sloshing Characteristics, Journal of Marine Science and Technology, Vol. 20, No. 4, 2015, pp. 765-775.

[22] Hou, L., Li, F., and Wu, C., A Numerical Study of Liquid Sloshing in A Two-Dimensional Tank Under External Excitations, Journal of Marine Science and Application, Vol. 11, 2012, pp. 305-310.

[23] Godderidge, B., Turnock, S., Tan, M., and Earl, Ch., An Investigation of Multiphase CFD Modelling of a Lateral Sloshing Tank, Computers and Fluids, Vol. 38, No. 2, 2009, pp. 183–193.

[24] Cao, X. Y., Ming, F. R., and Zhang, A. M., Sloshing in a Rectangular Tank Based on SPH Simulation, Applied Ocean Research, Vol. 47, 2014, pp. 241–254.

[25] Gotoh, H., Khayyer, A., Ikari, T., Arikawa, H., and Shimosako, K., On Enhancement of Incompressible SPH Method For Simulation of Violent Sloshing Flows, Applied Ocean Research, Vol. 46, 2014, pp. 104–115

[26] De Chowdhury, S., Sannasiraj, S. A., Numerical Simulation of 2D Sloshing Waves Using SPH with Diffusive Terms, Applied Ocean Research, Vol. 47, 2014, pp. 219–240.

[27] Shao, J. R., Li, H. Q., Liu, G. R., and Liu, M. B., An Improved SPH Method for Modeling Liquid Sloshing Dynamics, Computers & Structurest, Vol. 100-101, 2012, pp. 18–26.

[28] Acevedo-Malave, A., Modelling the Formation of Clusters of Drops by Means of the Flocculation and Coalescence Phenomena with Smoothed Particle hydrodynamics, CFD Letters, Vol. 5, No. 3, 2013, pp. 43-56.

[29] Dehnen, W., Aly, H., Improving Convergence in Smoothed Particle Hydrodynamics Simulations Without Pairing Instability, Monthly Notices of the Royal Astronomical Society, Vol. 425, No. 2, 2012, pp. 1068-1082.

[30] Bonet, J., Lok, T. S., Variational and Momentum Preservation Aspects of Smooth Particle Hydrodynamic Formulation, Computer Methods in Applied Mechanics and Engineering, Vol. 180, 1999, pp. 97-115.

[31] Aly, A. M., Lee, S. W., Numerical Simulations of Impact Flows with Incompressible Smoothed Particle

Hydrodynamics, Journal of Mechanical Science and Technology, Vol. 28, No. 6, 2014, pp. 2179-2188.

[32] Shamsoddini, R., Aminizadeh, N., Incompressible Smoothed Particle Hydrodynamics Modelling and Investigation of Fluid Mixing in A Rectangular Stirred Tank with A Free Surface, Chemical Engineering Communications, Vol. 204, No. 5, 2017, pp. 563–572.